energies

MDPI

Article

Intelligent Probability Estimation of Quenches Caused by Weak Points in High-Temperature Superconducting Tapes

Alireza Sadeghi, Zhihui Xu, Wenjuan Song and Mohammad Yazdani-Asrami *

Propulsion, Electrification & Superconductivity Group, James Watt School of Engineering, University of Glasgow, Glasgow G12 8QQ, UK
* Correspondence: mohammad.yazdani-asrami@glasgow.ac.uk

Abstract: Fluctuations in the critical current along the length of high-temperature superconducting (HTS) tapes manufactured in the form of coated conductors is a common manufacturing phenomenon. These fluctuations originate in the generation of weak points through the length of HTS tapes that may cause quenching later. By means of the propagation of quenches in HTS tapes, the reliability, stability, and the performance of the device and the system that contain HTS tapes could be seriously degraded. In this study, an artificial intelligence technique based on artificial neural networks (ANN) was proposed to estimate the probability of quenches in HTS tapes caused by weak points. For this purpose, six different HTS tapes were considered with different widths, total thicknesses, and thicknesses of sub-layers. Then, for each one of these tapes, different operating conditions were considered, where the operating temperature changed from 40 K to 80 K, in 1 K steps. Under each operating temperature, different operating currents were considered from 50% to 100% of tape critical current. All of these resulted in more than 5000 different data points. Then, for each of these data points, analytical modelling was performed to provide initial inputs and outputs for the ANN model. It should be noted that the performed simulations were conducted based on an analytical method that was experimentally validated in the literature. After that, a sensitivity analysis was conducted to select the hyperparameters and structure of the ANN-based model. The last step was to take advantage of the trained model, as a function in the MATLAB software package to estimate the probability of quenches in different case studies. The significant feature of the proposed model is the capability for estimating the probability of quenches under different operating temperatures and currents for different types of HTS tapes.

Keywords: artificial intelligence; critical current; quench; thermal runaway current; weak point

Citation: Sadeghi, A.; Xu, Z.; Song, W.; Yazdani-Asrami, M. Intelligent Probability Estimation of Quenches Caused by Weak Points in High-Temperature Superconducting Tapes. *Energies* **2023**, *16*, 193. https://doi.org/10.3390/en16010193

Academic Editors: Pawel Surdacki, Grzegorz Komarzyniec and Oleksandr Boiko

Received: 11 November 2022
Revised: 20 December 2022
Accepted: 21 December 2022
Published: 24 December 2022

1. Introduction

Implementation of high-temperature superconducting (HTS) tapes in large-scale power apparatuses is among the most promising scenarios to ensure the safe, reliable, and efficient operation of future power systems and electrified transportation units. HTS tapes could reduce the size, weight, loss, and total ownership cost of power devices while their efficiency and reliability are increased [1–3]. Although HTS tapes offer a wide range of advantages, their applications in airborne, marine, space, and terrestrial power systems face challenges such as cost, manufacturing issues, and all the challenges related to cryogenic operation, and thus the needs of a cryo-plant, the low energy efficiency of cryo-plants themselves, and complex integration and system engineering decisions. Among them, quenches and especially premature quenches are physical phenomena that could endanger the safe operation of superconducting devices in large-scale power applications. Quenching is defined as the transition of HTS tapes from a superconducting state to a non-superconducting state where HTS tapes show a high resistivity and may lead to burnouts of superconducting devices in severe cases if the devices are unprotected [4,5]. Indeed, quench analysis of

HTS tapes used in power devices plays a significant role in helping the commercialized application of HTS tapes for electric transportation units and power systems.

It should be noticed that weak points in HTS tapes are one of the origins of quenches, causing the local reduction in critical current, the local dissipation of power, thermal instability and thus quenches. In such points, the local critical current of HTS tapes is reduced to a value lower than the total critical current, and if this local critical current becomes lower than a threshold value and if this weak point is wide enough, quenches are highly possible/likely to occur. So, to analyze these weak points, there are multiple factors to be studied, including the local critical current, width of the weak point, operational temperature, and the operational current [6]. This is shown in Figure 1, which is a simple schematic of weak points in an arbitrary HTS tape with an yttrium barium copper oxide (YBCO) layer. Since the fluctuation of local critical current is a common phenomenon during the manufacturing process of HTS tapes, it is necessary for manufacturers to estimate the probability of quenches in their product, under different operational conditions. It is also necessary for users of HTS tapes to know how probable quenches that originate in local critical current fluctuations are during the design stages of HTS devices.

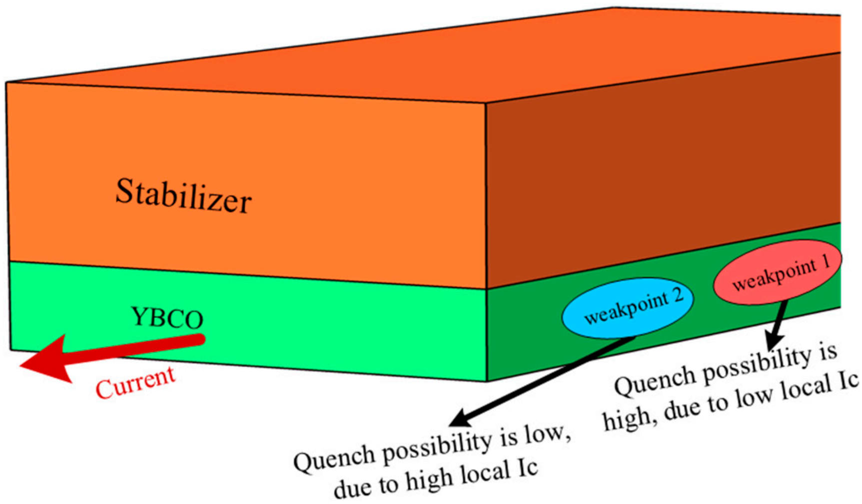

Figure 1. Weak points in YBCO tapes that increase the probability of quenches.

Many investigations were performed to analyze the quenches and their consequences in superconducting tapes, coils, and devices in the literature. These efforts could be categorized into four subclasses: experimental studies (ESs) [7–9], finite element-based methods (FEMs) [10–12], analytical approaches (Aps) [13–15], and intelligent methods (IMs). ESs are usually performed to characterize the quenches in superconductors under different thermal, mechanical, magnetic, electrical, and cryogenic conditions, but might be destructive to tape. FEMs and APs can be used for quench characterization in different superconducting devices and tapes. However, FEMs are usually too slow for real-time applications and APs are mostly specialized and characterized as being valid for one specific type of HTS tape that has gone through experimental tests, and so the outcomes of such models cannot be generally used for all types of HTS tapes or under all operating conditions. IMs are suitable for detecting and locating the quenches; however, there is a gap to develop a probability model of quenches. Such a probability model allows manufacturers to observe the performance of their products under different operating conditions. Additionally, a probability model could help engineers and researchers when designing an HTS device for a specific application. By accessing such a model, engineers could conceive which operational condition could reduce the risk of quenches as well as meeting the constraints of device operation.

In this paper, a method based on artificial neural networks (ANN) is proposed for the first time to calculate the probability of quenches in different YBCO tapes operating at different temperatures. For this purpose, data for six different YBCO tapes were extracted from Robinson Research Institute's open access database [16]. After that, an ANN is used to train a model to estimate the probability of quenches in these six tapes and then a plug and play code is proposed in MATLAB software package to estimate the quench probability. At last, three case studies are considered to test the performance of the function which is developed in quench detection.

2. Quench Probability Estimation

Due to micro-damages, manufacturing-related failures, local heating, and anisotropy of HTS materials, quenching can occur. The fluctuations of the critical current in HTS tapes results in an abrupt jump in voltage at these points. Consequently, by passing the operational current, which is higher than the local critical current, a local power dissipation occurs. If the width of the weak point is large enough and the local critical current is small enough, the dissipated power results in thermal instability of HTS tape, and so premature quenching takes place [14]. Each one of these weak points is probable to turn into a quench under a specific condition. The procedure of quench probability estimation deals with the probability of turning weak points into quenches. This can be affected by the operating temperature, operating current, structure of HTS tape, width of the weak points, value of local critical current in the weak points, and index value. To perform such estimation, it should be noted that weak points turn into a quench when the current passing through HTS tape surpasses a threshold value, known as thermal runaway current. Based on this, we consider different widths and minimum local critical currents for each one of HTS tapes, operating in pre-defined operational conditions. Then, for each one of cases of weak points, the width and minimum local critical current and thermal runaway current are calculated. After that, the number of cases where the operational current exceeds the value of thermal runaway current, known as quench events, is counted. Finally, the number of quench events is divided by the total cases and based on probability rules, the quench probability for each tape is calculated. According to [6,15], if the thermal operational current is higher than the runaway current, the occurrence of quenches is 100% certain. The thermal runaway current is calculated based on Equation (1) [15], which was experimentally validated in [6]:

$$I_{tr} = I_{cm} \left[\frac{k_{tape}(T_c - T_{op})}{I_{cm}\, e\, dx_{wp} E_c\, n(T)} \right]^{(n(T)+1)^{-1}} \tag{1}$$

where I_{tr} is the thermal runaway current, k_{tape} is the thermal conductivity of the HTS tape in $\frac{W}{m.\,K}$, I_{cm} is the minimum local critical current, T_c is the critical temperature, T_{op} is the operating temperature, e is Euler's number and is equal to 2.7183, dx_{wp} is the width of the weak point, E_c is the electric field criterion in μV/cm and $n(T)$ is the index value of the HTS tape at an operating temperature of T_{op}.

To gain a better understanding about the physical nature of quenches originating in weak points, Figure 2 is presented. Figure 2a shows the local characteristics of critical current in an HTS tape where the weak point has a width of dx_{wp} with the local critical current value of (I_{cm}), while the overall critical current of HTS tape is shown by (I_{c0}). Based on the characteristics of the weak point and with respect to Equation (1), an electrical threshold could be calculated known as thermal runaway current (I_{tr}). According to Figure 2b, if the operational current of the HTS tape (I_{op}), becomes higher than the thermal runaway current, the temperature of the HTS tape will enter the thermal runaway regime and would results in burnout of the HTS tape.

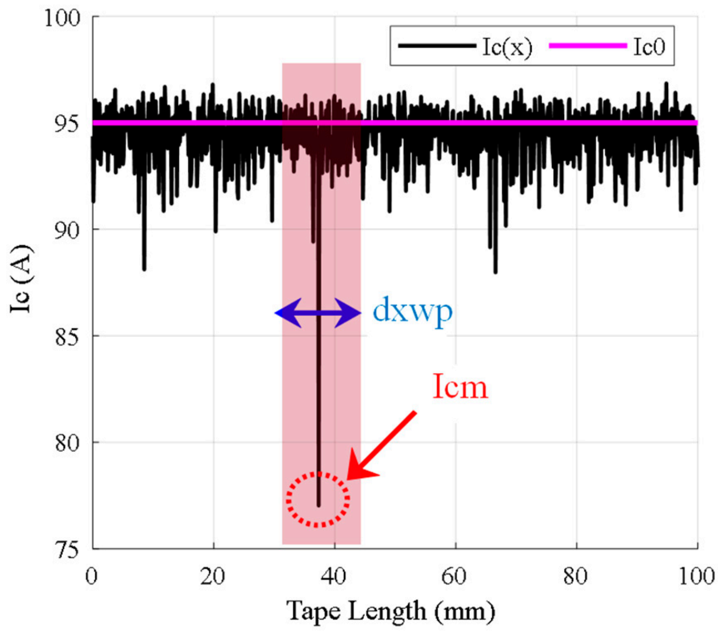

(**a**)

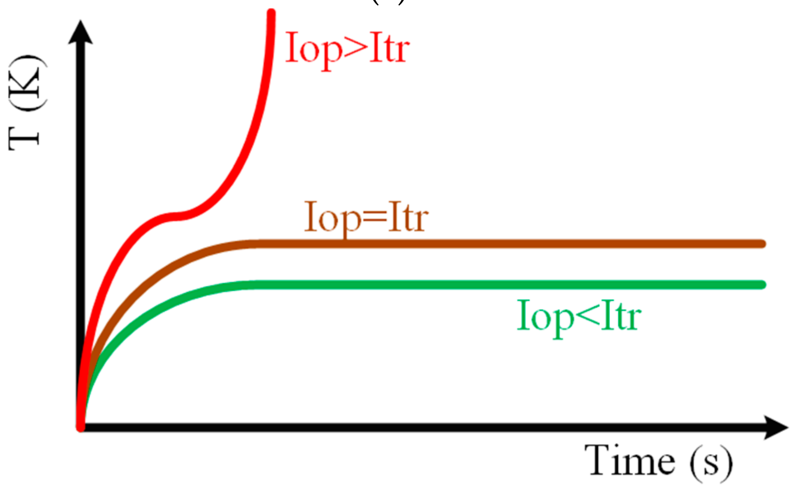

(**b**)

Figure 2. Illustration of different parameters and factors for defining thermal runaway current, (**a**) local critical current of an arbitrary HTS tape. (**b**) Temperature characteristic of HTS tape under different operational conditions and weak points.

According to Equation (1), the thermal runaway current in each HTS tape which could result in quenching can be changed based on variations in the minimum local critical current (I_{cm}), operating temperature (T_{op}), tape properties and specifications, and the width of the weak point (dx_{wp}). Equation (1) presents the electrical limitation for each HTS tape and does not directly calculate the probability of quenches in HTS tapes. To find this, firstly we have to acquire the thermal runaway current for all possible cases of I_{cm} and dx_{wp} under a specific operating current and temperature. After these steps, the quench probability is calculated based on Equation (2) and by using the value of the normalized operating current I_{op}/I_c:

$$P_q = \frac{n_q}{n_{tot}} \times 100 \tag{2}$$

where P_q is the quench probability in %, n_q is the number of events in which the operating current is higher than the thermal runaway current, and n_{tot} is the total number of states. Events in probability can be defined as a set of outcomes of a random experiment.

Next, n_{tot} is calculated based on Equation (3) and n_q is calculated based on Equation (4):

$$n_{tot} = n_x \times n_c \quad (3)$$

$$n_q = \sum state_i \; where \; I_{op_i} \geq I_{tr_i} \quad (4)$$

where n_x is the total number of considered widths for weak points, and n_c is the total number of $I_{cm}/I_{coveral}$. Additionally, $state_i$ refers to the ith state where operating current is higher than the calculated thermal runaway current based on values considered for dx_{wp} and I_{cm}. To calculate this, the width of weak points is considered to be between 0.05 mm and 20 mm, as proposed in [15], and n_c is considered to be 0.5 to 1, which is due to the fact that the safety margin of the critical current for HTS tapes in large-scale power applications is usually between 0.4 and 0.6, which means that no quenching is probable for normalized operating currents lower than this range.

Figure 3 shows the quench probability flowchart for the proposed model in this paper. Firstly, operating conditions and tape structure are received, and then initial values for the width of the weak point (Wi) and the ratio of the minimum local critical current to the overall critical current (Ri) is considered. After that, for these values, the thermal runaway current is calculated and then one has to check if thermal runaway current is lower than operating current or not. If thermal runaway current is lower than operating current, number of quench events (nq) is counted, on the other hand number of non-quench states (nnq) is counted. At the next stage, Ri and Wi must be increased based on a step related to Ri, known as dr and another step related to with, known as dW. After increasing the minimum critical current in the weak point and width of the weak point, it should be checked whether the considered ratio and width are higher than the upper bound of these values or not. In the last step, quench probability is calculated based on nnq and nq values.

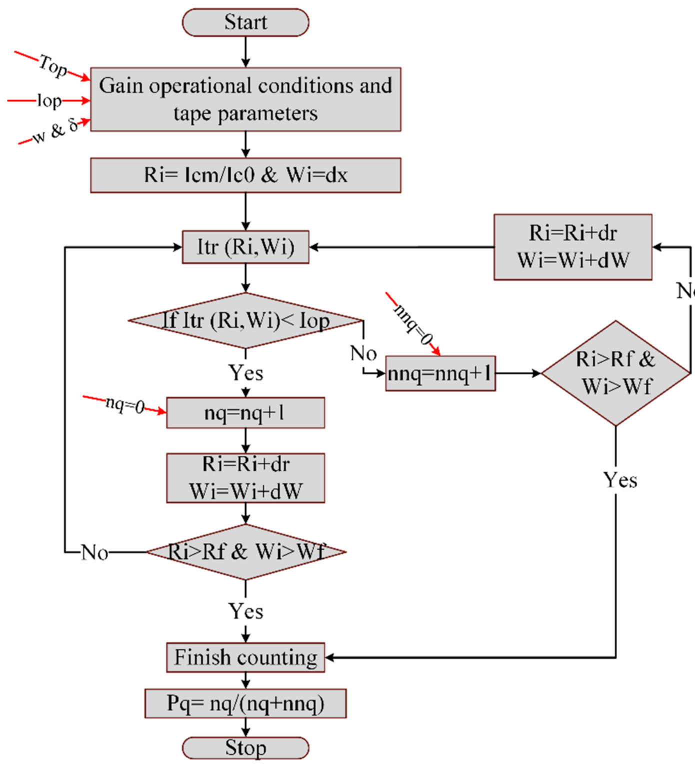

Figure 3. The flowchart of the proposed model to calculate the probability of quenches.

3. ANN Model Development

In recent years, artificial intelligence (AI) techniques, especially machine learning (ML) methods, have attracted widespread attention for their successful applications in many engineering fields. In superconductivity, AI techniques have been applied to address design [17], condition monitoring [18], control [19], and modelling [20] issues for large-scale applications. ANN is an AI-based technique that is used to characterize nonlinear and complex characteristics through given inputs and outputs to minimize objective function that is given in Equation (5) [21]:

$$F_\varepsilon = \frac{1}{2}\sum_{i=1}^{n_d}(d_i - y_i)^2 = \frac{1}{2}\sum_{i=1}^{n_d} e_i^2 \tag{5}$$

where F_ε is the objective function, n_d is the number of data, d_i is the desired value, y_i is the predicted/estimated value, and e_i is the error value.

Any ANN model is divided into three layers, the input layer, the hidden layers, and the output layer, as shown in Figure 4. The neurons of the input layer are primarily used to receive the data from external input resources. Activation functions are used to generate nonlinear variations in neural networks, and the function is used to map a feature to a new feature space which is more conducive to training [22]. The activation function is often configured as a bounded monotonic function. Neurons process the input signals and the result in the outputs for both the hidden and output layers. The hidden layer in ANN supplies the computing ability and processing power to produce the network output [21].

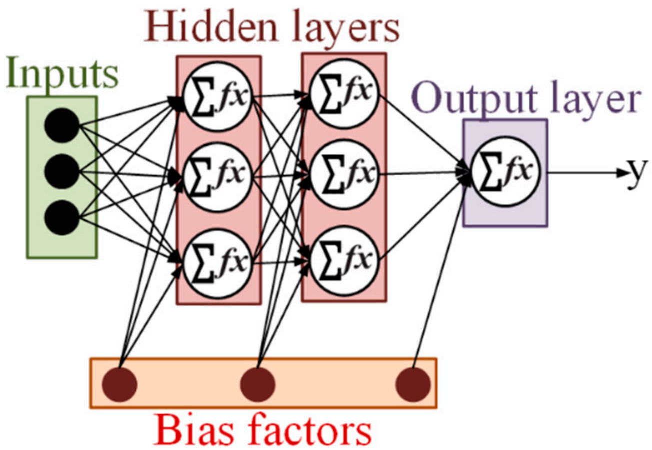

Figure 4. General structure for an ANN-based model.

The calculation from the input layer to the first hidden layer of ANN can be shown as expressed in Equation (6) [21]:

$$H_{1j} = f\left(\textstyle\sum_{i=1}^{n} w_{ij}x_i + b_j\right) \tag{6}$$

where $j = 1,2\ldots N$. H_{hj} is the jth node in the first hidden layer. The w_{ij} is the connection weight from the ith node of the input layer to the jth node of the first hidden layer and x_i indicates the input from ith node. The b_j is bias of jth node in the first hidden layer.

When the output transfers to next hidden layer, the output can be calculated by Equation (7) [21]:

$$H_{hj} = f\left(\textstyle\sum_{i=1}^{n} w_{ij}x_i\right) \tag{7}$$

where $j = 1,2\ldots N$, $h = 1,2\ldots M$. H_{hj} is the jth node in the hth hidden layer.

When the output of the hidden layer has been calculated, the calculation from hidden layer to output layer is as expressed in Equation (8) [21]:

$$O_k = f\left(\sum_{i=1}^{n} w_{jk} H_{Mj} + b_k\right) \quad (8)$$

where $j = 1, 2 \ldots N$, $k = 1, 2 \ldots m$. w_{jk} is the connection weight from the jth node of the last hidden layer to the kth nodes of output layer and H_{Mj} indicates the output from the jth node of the last hidden layer. The b_k is the bias factor of the kth node in the output layer.

In the analysis process, the sample data are divided into a training set, a validation set and a testing set, as shown in Figure 5. The training set fits the model and derives the neurons' built-in parameters. The model's hyper-parameters are modified using the validation set, and a preliminary evaluation of the model's performance is conducted. The test set evaluates the performance of the final model and its ability to classify the data [23]. Finally, it should be noted that thermal run-away current is modelled only in analytical equations and not in the ANN-based model; therefore, the ANN model only predicts the quench probability based on the tape structure and operating condition.

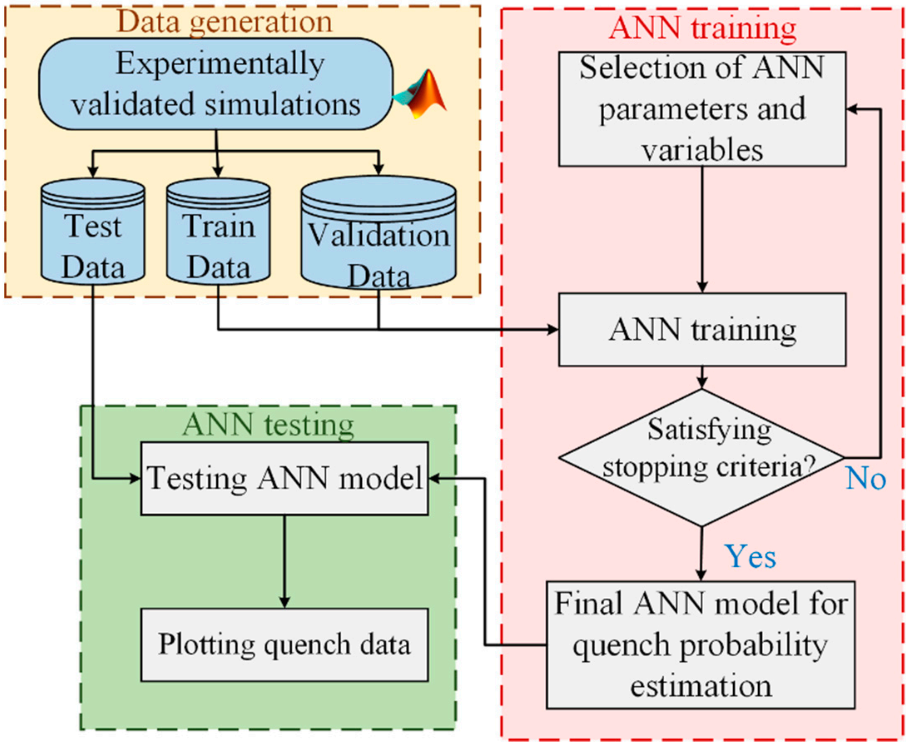

Figure 5. The structure of the proposed ANN-based model for quench probability estimation.

For quench probability estimation, eight inputs for the ANN-based model were considered in this paper, namely, operating current, operating temperature, tape width, tape thickness, stabilizer thickness, superconducting layer thickness, shield thickness, and substrate thickness. It should be noted that the training data as well as validation and test data are provided based on the analytical method, as explained in Section 2. The importance of developing an ANN-based model for quench probability estimation, instead of continuing to work with the analytical model, is due to the adaptability and updatability of the ANN model. This means that the proposed ANN-based model could be updated and adapted in future based on any new data fed into the model. This is an excellent aspect for any model to be fitted with new requirements and properties of HTS tapes or even HTS devices.

The root mean squared error ($RMSE$) and Pearson correlation coefficient (R) are used to evaluate the error and accuracy of the quench probability estimation, which are formulated as in Equations (9) and (10) [24]:

$$RMSE = \sqrt{\sum_{k=1}^{n_s} \frac{(d_k - y_k)^2}{n_s}} \tag{9}$$

$$R = \frac{\sum_{k=1}^{n_s} (d_k - \overline{d})(y_k - \overline{y})}{\sqrt{\sum_{k=1}^{n_s} (d_k - \overline{d})^2 \sum_{k=1}^{n_s} (y_k - \overline{y})^2}} \tag{10}$$

4. Results and Discussion

Based on the I_c and index value data presented in [16] for different temperature ranges, we decided to develop our ANN-based model for six different tapes, tabulated in Table 1 [25]. The temperature range was selected to be 40 K to 80 K for all tapes and the I_{op}/I_c ratio was from 0.5 to 1, as discussed before to consider the safety margin. This ratio plays a significant role during the design of HTS devices such as cables, machines, transformers, SFCLs, SMESs, etc., henceforth referred to in this paper as o. It should be mentioned that the 85% value for the operating factor is over-conservative and a weak spot is less likely with this local critical current. However, we considered values of less than 85% for the operating factor to observe the specific trend for quench probability. Additionally, this wide range of operating factors could increase the adaptability of the developed ANN-based model and make it able to react under all possible circumstances/consequences. By doing this, the proposed model is capable of estimating the probability of quenches for different superconducting tapes while the temperature effect is adjusted in the model. Please note that further tape samples can be easily added to this model in future, as it was designed to be quite flexible.

Table 1. Geometrical properties of HTS tapes used for quench probability estimation in the ANN model.

Manufacturer	Width (mm)	Thickness (μm)
AMSC Amperium® 2G HTS	12	100
Fujikura FESC 2G HTS	4	106
Shanghai Creative Superconductor	4	60
SuNAM SAN04200	4	170
SuperOx YBCO	4	150
THEVA	10	110

4.1. Sensitivity Analysis on ANN Structure and Hyperparameters

There are two important hyper- or controlling parameters in each ANN model, namely the number of neurons and the number of hidden layers. Choosing the best values of the ANN model hyperparameters will reduce the error and increase the accuracy of the whole quench probability estimation procedure. Figure 6a shows the impact of the aforementioned hyperparameters on the RMSE of estimations. As can be seen, the increase in the number of hidden layers and the number of neurons results in RMSE reduction from 10% to less than 0.001%. On the other hand, Figure 6b illustrates the impact of the hidden layers and neuron number on the R value of estimations. Based on the results shown in Figure 5, the number of hidden layers (nH) is selected to be seven, which results in the lowest RMSE value and the highest R value, among other things. Additionally, the number of neurons is selected to be 17, which reduces the RMSE value to the lowest possible value and R to highest possible value. It should be also mentioned that increasing the number of neurons and nH to be more than the selected values does not change the RMSE and R values significantly, while the training time will be dramatically increased. In this stage, the training method was based on the Levenberg–Marquardt algorithm explained in [26]. For the sake of clarification about the training time of each case study, Figure 7 is presented. In this figure, it can be seen that the training time is increased by increasing the number of neurons and the number of hidden layers, while in all cases studies, the training time remains lower than 90 s. It should be mentioned that the computational resources that have been used for gaining such a time are as follows:

- 16 GB DDR3 RAM
- AMD Ryzen 7 1700 eight-core processor unit (CPU).

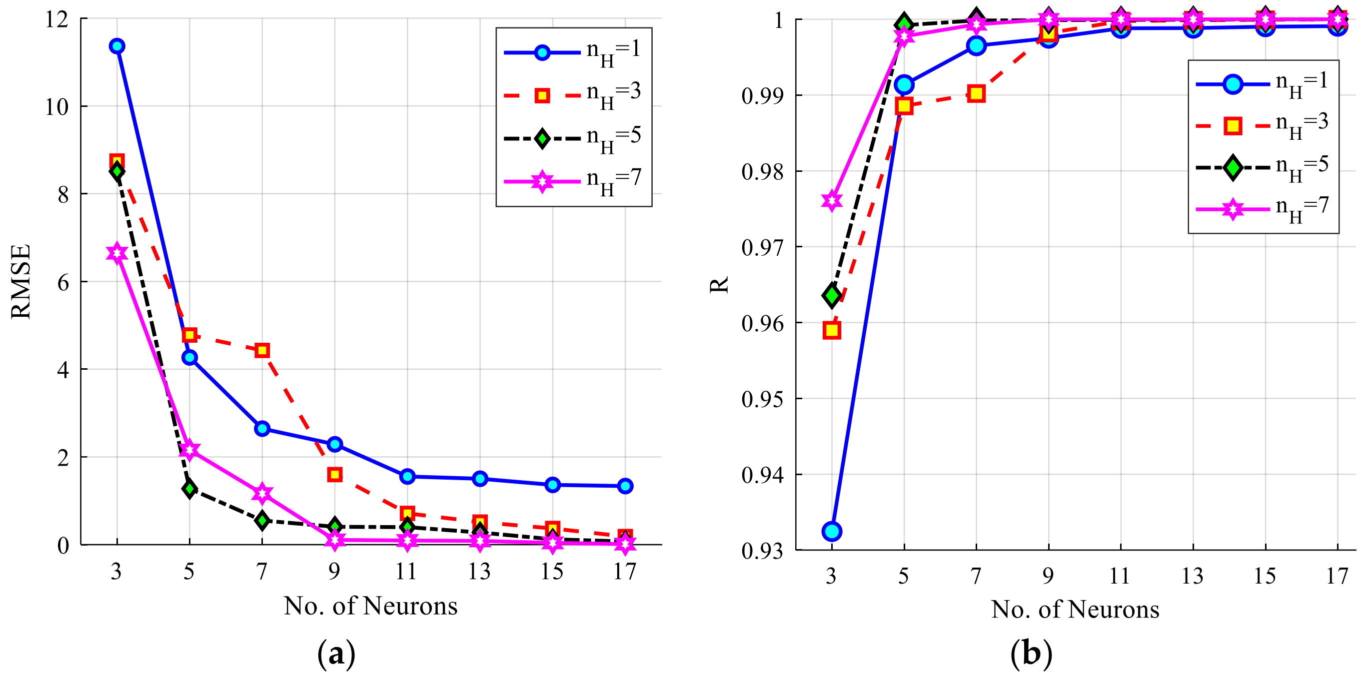

Figure 6. Sensitivity analysis on the performance of the ANN-based model with respect to the variation of (**a**) RMSE by changing the structure of ANN, (**b**) R value by changing the structure of ANN.

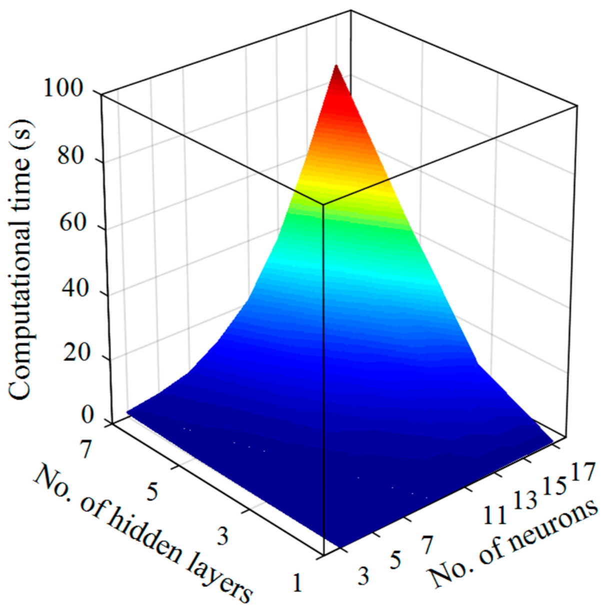

Figure 7. The changes in training time with respect to the changes in the hidden layer number and neuron number.

This is just a personal computer, and indeed if one uses high-performance computation resources, this training time can be shorter than a second.

4.2. Accuracy of ANN-Based Model

After tuning the hyperparameters, Figure 7 shows the estimated probability versus expected probability. The more accurate the estimation is, the more the distribution of data points in Figure 8 must be aligned to the $y = x$ line. The R value is about 0.99999, showing the high capability of the ANN model in estimating the quench probability.

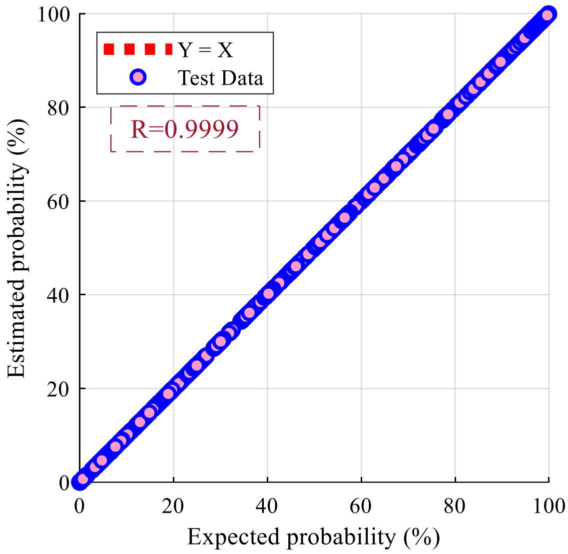

Figure 8. Regression for quench probability estimation by proposed structure of ANN.

Figure 9 shows the estimated values and expected (real) values in the solid black line and dotted red line, respectively. As can be seen in this figure, the estimated values are in excellent agreement with the real values. This can also be seen for the absolute error in Figure 8, which is shown by the solid blue line. The absolute error shows that the maximum error between estimated and real values is 1.35%. Additionally, most of the absolute error data are in range of -0.2% to 1.2%, which indicates the high accuracy of the model.

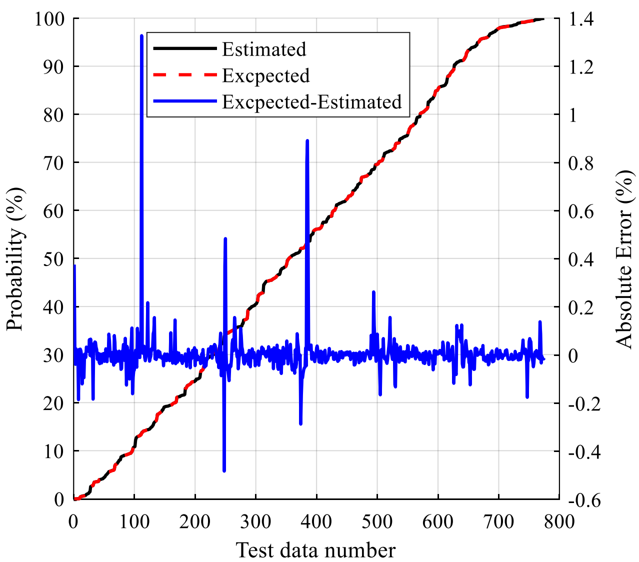

Figure 9. Comparing the results of the estimated quench probability versus expected values based on the absolute error index.

Figure 10 depicts the estimated quench probability versus temperature and operating current. Regardless of quench probability, the figure shows that the lower the temperature gets, the Ic value of each HTS tape increases, and thus HTS tapes can carry a higher current at lower temperatures. On the other hand, the low possibility of quenching (lower than 30%) is distributed more in areas with low temperature and low current. This is because of the nature of HTS tapes, where in lower temperatures, Ic is increased and if the passing current remains lower that the Ic value (especially 50% lower than Ic), the probability of quenching is reduced significantly.

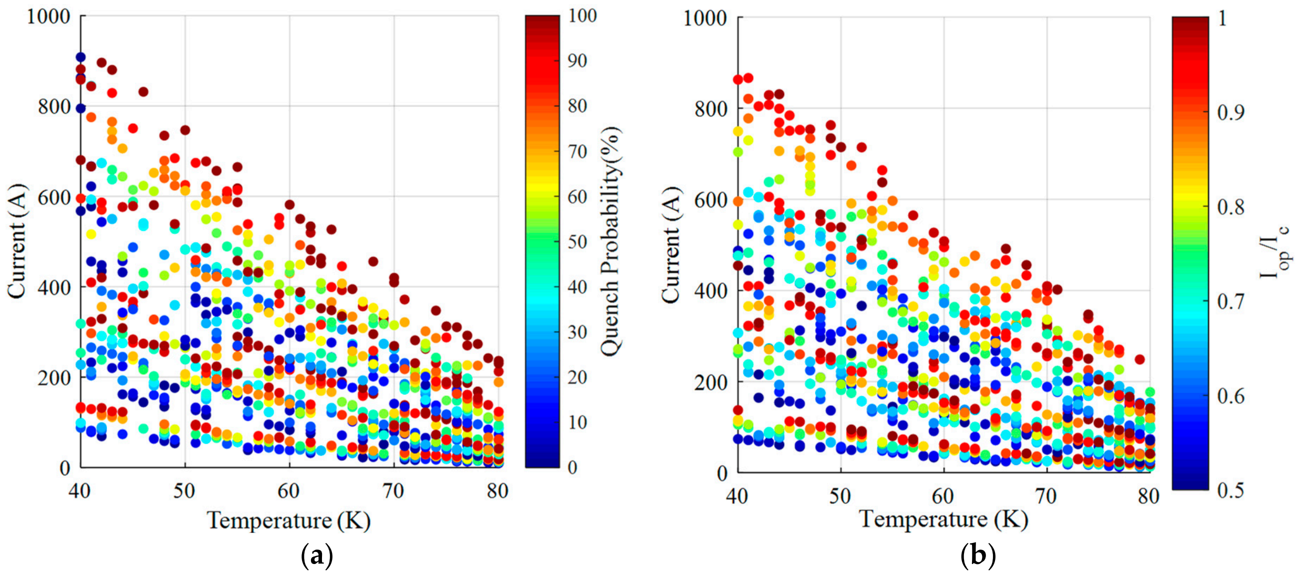

Figure 10. Current-temperature distribution of test points. (**a**) Based on quench probability. (**b**) Based on normalized operating current.

4.3. Case Studies: MATLAB Function

To avoid a long computation procedure, once the model is trained, we developed a MATLAB ANN function that operates based on the trained ANN model to estimate quench probability. To test the performance of the ANN function, we tested three different tapes and fed their operating conditions into the developed MATLAB function. As shown in Figure 11a, firstly, the operating temperature is established by the program. After that, as illustrated in Figure 11b, the type of HTS tape must be selected. Three case studies are analyzed under different operating condition including current and temperature for each tape. For each tape, two temperatures are considered—50 K, which represents an ideal thermal condition which is much lower than the critical temperature of HTS tapes, and 80 K, which represents a near-critical temperature for HTS tapes. It should also mentioned be that for all cases, the minimum local critical current is considered to be 50% lower than the overall critical current. This means that in the worst-case scenario, local critical currents are 50% lower than the overall critical current.

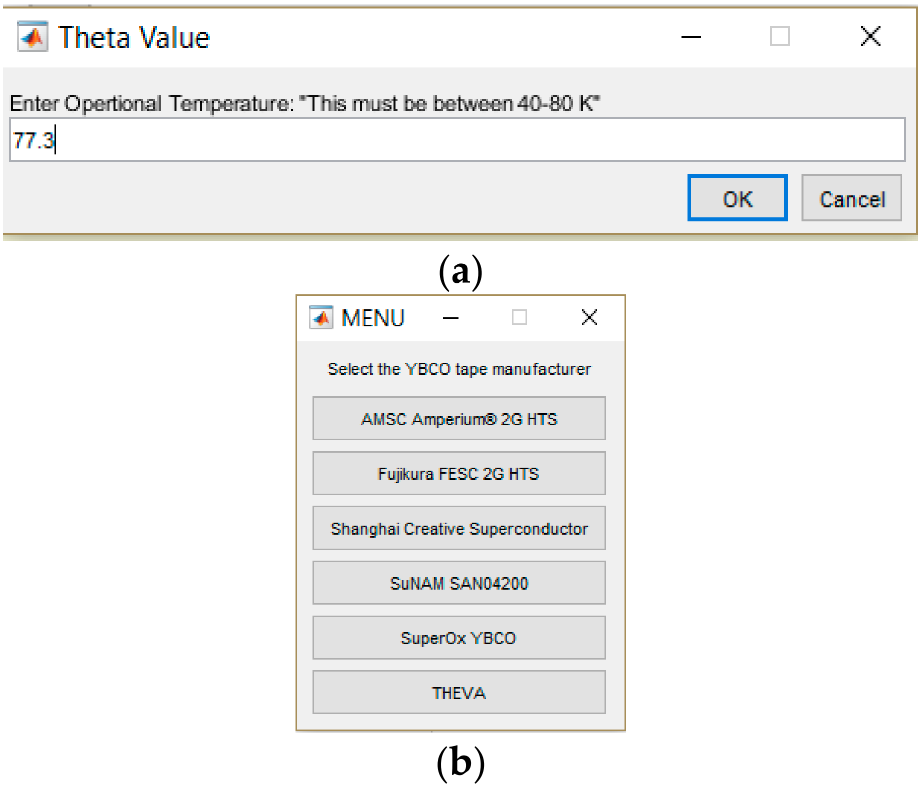

Figure 11. Quench probability calculation steps for different HTS tapes, (**a**) the related window to gain operational temperature. (**b**) the related window to select the type of HTS tape.

As shown in Table 2, for all HTS tapes and under all temperatures, the quench probability under 50% loading is equal to zero. In this scenario, the thermal runaway current is always higher than the operating current, and quenching is absolutely impossible. On the contrary, when a fault current passes through HTS tape with a three times higher amplitude than the critical current, representing fault currents in superconducting devices, quenching is 100% probable. For full loading conditions, there is a quench probability of 21% to 27%. This means that under assumed condition, regardless of the application of HTS tapes, if they operate at full load, they will probably quench. This is considered the worst-case scenario when *Icm* is 50% lower than overall critical current. If *Icm* increases to just 55%, the quench probability will be 12% to 16%, and if *Icm* increases to 60%, the probability will be changed to 2% to 6%. For overloading conditions, the quench probability is higher than 80%, and this means that quenching is highly probable in this scenario. If the worst-case scenario of local critical current reduces to 90% of the overall critical current, the quench probability is still 28%. This means that in overloading conditions, quenching is highly probable. Regarding the test time of the proposed method, it can be seen that it has values about 1 to 4 ms, which is an excellent choice for real-time condition monitoring of superconducting devices.

Table 2. The test performance of the proposed ANN model for quench probability estimation.

	Current Level	Operating Factor	HTS Tape-Shanghai Creative Superconductor		HTS Tape-SuNAM SAN04200		HTS Tape-THEVA	
			50 K	80 K	50 K	80 K	50 K	80 K
Quench probability (%)	50% loading	0.3	0	0	0	0	0	0
	100% loading	0.6	21.29	22.43	24.89	27.45	23.12	26.36
	150% loading	0.9	85.61	88.03	90.37	94.11	88.81	93.43
	Fault current	3	100	100	100	100	100	100
Test time (ms)	50% loading	0.3	3.58	2.81	2.05	1.19	4.28	1.37
	100% loading	0.6	2.56	2.51	3.75	2.62	3.01	3.29
	150% loading	0.9	4.54	1.35	1.74	3.43	3.55	3.99
	Fault current	3	1.15	3.91	4.54	4.43	2.67	2.84

Figure 12 shows the impact of the worst-case scenario of local critical current on the quench probability at different temperatures, for an operating factor of 0.6 and Shanghai Creative Superconductor HTS tape. By increasing the local critical current from 0.5 to 0.7, the quench possibility increases from 4% to 19%. Thus, when one designs a superconducting device such as an HTS machine, an HTS cable, an HTS transformer, etc., one must take the lowest value of local critical current into consideration. This value could be affected by the operating temperature, self and external magnetic fields, and applied strain.

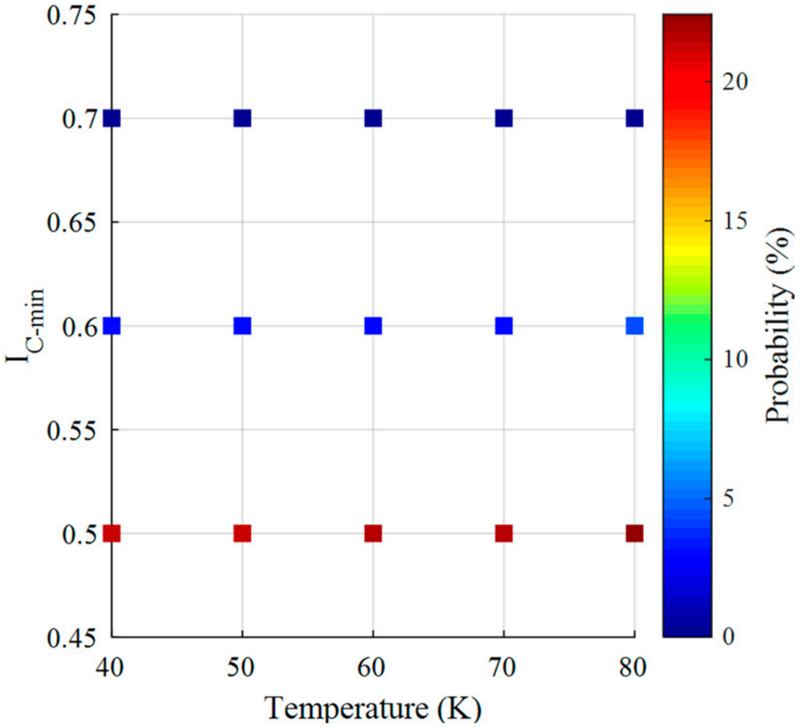

Figure 12. The impact of minimum critical current on the quench probability of Shanghai Creative Superconductor HTS tape.

5. Conclusions

Quenching is among the most significant issues of high-temperature superconducting (HTS) tapes in large-scale power applications that could result in their thermal runaway and even burnout. In this paper, an artificial neural network (ANN)-based surrogate model is proposed for the first time to enable the estimation of quench probability in various HTS tapes. For this purpose and the adaptability of the model in future investigations, an ANN-based model is used to build an intelligent method that is capable of estimating the probability of quenches in different HTS tapes. Then, a function is built in the MATLAB software package as a code that can be used as a plug and play software in other applications such as coils, cables, etc., during their condition monitoring and design stages. By having such a model, the manufacturer can observe the probability of quenches in the produced HTS tape and can reduce it by improving the local critical current value of the HTS tape.

The most important findings and research outcomes of this paper are:

- The ANN-based model is capable of estimating quench probability for different types of HTS tapes with 4 mm, 10 mm, and 12 mm width.
- It turned out that the ANN-based surrogate model with 7 hidden layers and 17 neurons in each layer is the best structure for ANNs to estimate the probability of quenches.
- The proposed ANN-based model is a highly accurate model with an accuracy higher than 99.9%.
- The probability of quenches depends highly on the minimum value of local critical currents, especially in full load condition of HTS tapes
- Under 50% loading conditions of HTS tapes (i.e., I_{op} = 0.3I_c), quenching is completely impossible.
- Under overloading conditions of HTS tapes (i.e., I_{op} = 0.9I_c), quenching is highly possible, at a probability of 70% to 90%, based on different HTS tapes and temperatures.
- Under fault conditions (i.e., I_{op} = 3I_c), the probability of quenching is 100%.
- As the future work, the impact of magnetic field amplitude and its orientation on the probability of quenching in HTS tapes can be integrated into the presented model. Additionally, adding other types of quenches to this model can be conducted in future.

Author Contributions: Conceptualization, A.S. and M.Y.-A.; methodology, A.S. and M.Y.-A.; software, A.S. and Z.X.; validation, A.S. and M.Y.-A.; formal analysis, A.S. and Z.X.; investigation, A.S. and M.Y.-A.; resources, M.Y.-A.; data curation, A.S. and Z.X.; writing—original draft preparation, A.S. and Z.X.; writing—review and editing, M.Y.-A.; visualization, A.S.; supervision, W.S. and M.Y.-A.; project administration, W.S. and M.Y.-A.; funding acquisition, W.S. and M.Y.-A. All authors have read and agreed to the published version of the manuscript.

Funding: This research received no external funding.

Data Availability Statement: Not applicable.

Acknowledgments: Networking support provided by the European Cooperation in Science and Technology, COST Action CA19108 (Hi-SCALE) is acknowledged.

Conflicts of Interest: The authors declare no conflict of interest.

References

1. Marchionini, B.G.; Yamada, Y.; Martini, L.; Ohsaki, H. High-Temperature Superconductivity: A Roadmap for Electric Power Sector Applications, 2015–2030. *IEEE Trans. Appl. Supercond.* **2017**, *27*, 0500907. [CrossRef]
2. Musso, A.; Angeli, G.; Bocchi, M.; Luigi, P.; Breschi, M. A Method to Quantify Technical-Economic Aspects of HTS Electric Power Cables. *IEEE Trans. Appl. Supercond.* **2022**, *32*, 4803516. [CrossRef]
3. Guarino, R.; Wesche, R.; Sedlak, K. Technical and economic feasibility study of high-current HTS bus bars for fusion reactors. *Phys. C Supercond. Appl.* **2021**, *592*, 1353996. [CrossRef]
4. Hoang, D.; Boffo, C.; Tran, N.; Krave, S.; Kazi, S.; Stoynev, S.; Marinozzi, V. Intelliquench: An Adaptive Machine Learning System for Detection of Superconducting Magnet Quenches. *IEEE Trans. Appl. Supercond.* **2021**, *31*, 4900805. [CrossRef]
5. Song, W.; Pei, X.; Alafnan, H.; Xi, J.; Zeng, X.; Yazdani-Asrami, M.; Xiang, B.; Liu, Z. Experimental and Simulation Study of Resistive Helical HTS Fault Current Limiters: Quench and Recovery Characteristics. *IEEE Trans. Appl. Supercond.* **2021**, *31*, 5601106. [CrossRef]
6. Gömöry, F.; Šouc, J. Stability of DC transport in HTS conductor with local critical current reduction. *Supercond. Sci. Technol.* **2021**, *34*, 025005. [CrossRef]
7. Bansal, G.; Yanagi, N.; Hemmi, T.; Takahata, K.; Mito, T. Experimental Investigation of the Minimum Propagation Currents and Quench Characteristics of LTS/HTS Hybrid Conductors. *IEEE Trans. Appl. Supercond.* **2007**, *17*, 2474–2477. [CrossRef]
8. Zhou, J.; Schwartz, J. Effect of heaters on the measurement of normal zone propagation velocity on short YBCO conductors. *Phys. C Supercond.* **2021**, *583*, 1353848. [CrossRef]

9. Xu, Y.; Chen, G.; Feng, T.; Cai, Z.; Yue, Y.; Ren, L.; Tang, Y. Experimental Study on the Performance Change of YBCO Tapes Under Repeated Overcurrent. *IEEE Trans. Appl. Supercond.* **2020**, *30*, 8000310. [CrossRef]
10. Majoros, M.; Sumption, M.D.; Zhang, D.; Collings, E.W. Quench Measurements in a YBCO Pancake Coil at 77 K and 4.2 K in Magnetic Fields up to 10 Tesla. *IEEE Trans. Appl. Supercond.* **2019**, *29*, 4600805. [CrossRef]
11. Riva, N.; Richard, S.; Sirois, F.; Lacroix, C.; Dutoit, B.; Grilli, F. Overcritical Current Resistivity of YBCO-Coated Conductors Through Combination of PCM and Finite-Element Analysis. *IEEE Trans. Appl. Supercond.* **2019**, *29*, 6601705. [CrossRef]
12. Cavallucci, L.; Breschi, M.; Ribani, P.L.; Yang, Y. Electrothermal Modeling of Quench in REBCO Roebel Cables. *IEEE Trans. Appl. Supercond.* **2018**, *28*, 4703405. [CrossRef]
13. Kang, R.; Uglietti, D.; Wesche, R.; Sedlak, K.; Bruzzone, P.; Song, Y. Quench Simulation of REBCO Cable-in-Conduit Con-ductor With Twisted Stacked-Tape Cable. *IEEE Trans. Appl. Supercond.* **2020**, *30*, 5700107. [CrossRef]
14. Gömöry, F.; Šouc, J. Current–Voltage Curve of the High Temperature Superconductor with Local Reduction of Critical. *Supercond. Sci. Technol.* **2021**, *34*, 12LT01. [CrossRef]
15. Gömöry, F.; Souc, J. Probability of Premature Quenching of HTS Coil Due to Local Reduction of Critical Current. *IEEE Trans. Appl. Supercond.* **2022**, *32*, 4604005. [CrossRef]
16. Robinson HTS Wire Critical Current Data Base. Available online: https://htsdb.wimbush.eu/ (accessed on 10 October 2022).
17. Koster, R.; Binder, A. Multi-Objective Optimization of a Direct-Drive Wind Turbine Generator With HTS Excitation Winding. *IEEE Trans. Appl. Supercond.* **2022**, *32*, 5200508. [CrossRef]
18. Yazdani-Asrami, M.; Sadeghi, A.; Song, W.; Madureira, A.; Murta-Pina, J.; Morandi, A.; Parizh, M. Artificial intelligence methods for applied superconductivity: Material, design, manufacturing, testing, operation, and condition monitoring. *Supercond. Sci. Technol.* **2022**, *35*, 123001. [CrossRef]
19. Tsotsopoulou, E.; Karagiannis, X.; Papadopoulos, P.; Dyśko, A.; Yazdani-Asrami, M.; Booth, C.; Tzelepis, D. Time-Domain Protection of Superconducting Cables Based on Artificial Intelligence Classifiers. *IEEE Access* **2022**, *10*, 10124–10138. [CrossRef]
20. Yazdani-Asrami, M.; Sadeghi, A.; Seyyedbarzegar, S.; Song, W. DC Electro-Magneto-Mechanical Characterization of 2G HTS Tapes for Superconducting Cable in Magnet System Using Artificial Neural Networks. *IEEE Trans. Appl. Supercond.* **2022**, *32*, 4605810. [CrossRef]
21. Graupe, D. *Principles of Artificial Neural Networks*; World Scientific Publishing: Singapore, 2013.
22. Tharsanee, R.M.; Soundariya, R.S.; Kumar, A.S.; Karthiga, M.; Sountharrajan, S. *Data Science for COVID-19*; Academic Press: Cambridge, MA, USA, 2021.
23. Puig-Arnavat, M.; Bruno, J. *Recent Advances in Thermo-Chemical Conversion of Biomass*; Elsevier: Amsterdam, The Netherlands, 2015.
24. Yazdani-Asrami, M.; Sadeghi, A.; Seyyedbarzegar, S.M.; Saadat, A. Advanced experimental-based data-driven model for the electromechanical behavior of twisted YBCO tapes considering thermomagnetic constraints. *Supercond. Sci. Technol.* **2022**, *35*, 054004. [CrossRef]
25. Tsuchiya, K.; Kikuchi, A.; Terashima, A.; Norimoto, K.; Uchida, M.; Tawada, M.; Masuzawa, M.; Ohuchi, N.; Wang, X.; Takao, T.; et al. Critical current measurement of commercial REBCO conductors at 4.2 K. *Cryogenics* **2017**, *85*, 1–7. [CrossRef]
26. Krogh, A. What Are Artificial Neural Networks? *Nat. Biotechnol.* **2008**, *26*, 195–197. [CrossRef] [PubMed]